Microhydration Effects on the Encapsulation of Potassium Ion by Dibenzo-18-Crown-6

Yoshiya Inokuchi,[‡,*] Takayuki Ebata,[‡] Thomas R. Rizzo[†] and Oleg V. Boyarkin[†]

Department of Chemistry, Graduate School of Science, Hiroshima University, Higashi-Hiroshima, Hiroshima 739-8526, Japan and Laboratoire de Chimie Physique Moléculaire, École Polytechnique Fédérale de Lausanne, Lausanne CH-1015, Switzerland

E-mail: y-inokuchi@hiroshima-u.ac.jp

Abstract

We have measured electronic and conformer-specific vibrational spectra of hydrated dibenzo-18-crown-6 (DB18C6) complexes with potassium ion, K^+•DB18C6•$(H_2O)_n$ (n = 1–5), in a cold, 22-pole ion trap. We also present for comparison spectra of Rb^+•DB18C6•$(H_2O)_3$ and Cs^+•DB18C6•$(H_2O)_3$ complexes. We determine the number and the structure of conformers by analyzing the spectra with the aid of quantum chemical calculations. The K^+•DB18C6•$(H_2O)_1$ complex has only one conformer under the conditions of our experiment. For K^+•DB18C6•$(H_2O)_n$ with n = 2 and 3, there are at least two conformers even under the cold conditions, whereas Rb^+•DB18C6•$(H_2O)_3$ and Cs^+•DB18C6•$(H_2O)_3$ each exhibit only one isomer. The difference can be explained by the optimum matching in size between the K^+ ion and the crown cavity; since the K^+ ion can be deeply encapsulated by DB18C6 and the interaction between the K^+ ion and the H_2O molecules becomes weak, different kinds of

hydration geometries can occur for the K^+•DB18C6 complex, giving multiple conformations in the experiment. For K^+•DB18C6•$(H_2O)_n$ (n = 4 and 5) complexes, only a single isomer is found. This is attributed to a cooperative effect of the H_2O molecules on the hydration of K^+•DB18C6; the H_2O molecules form a ring, which is bound on top of the K^+•DB18C6 complex. According to the stable structure determined in this study, the K^+ ion in the K^+•DB18C6•$(H_2O)_n$ complexes tends to be pulled largely out from the crown cavity by the H_2O molecules with increasing n. Multiple conformations observed for the K^+ complexes will have an advantage for the effective capture of the K^+ ion over the other alkali metal ions by DB18C6 because of entropic effects on the formation of hydrated complexes.

Keywords: alkali metal ions, 18-crown-6, encapsulation, water, crown ether, infrared, ion trap, electrospray, solvent effect

*To whom correspondence should be addressed.

[‡]Hiroshima University

[†]École Polytechnique Fédérale de Lausanne

1. Introduction

Crown ethers are among the most common host molecules in supramolecular chemistry and are extensively used as phase transfer catalysts in organic synthesis. Despite their wide use, the origin of their functionality has not been fully understood at the molecular level. For example, 18-crown-6 (18C6) selectively captures K^+ in a water solution of different alkali metal ions.[1,2] This ability of selective encapsulation has been explained mainly in terms of optimal size matching between the cavity of crown ethers and guest species, based on X-ray analysis.[1,3] Focusing on the alkali metal ion–18C6 complexes, the ion selectivity can be expressed by the following metal exchange reaction:[4,5]

$$K^+\bullet 18C6 + M^+ \rightleftharpoons M^+\bullet 18C6 + K^+ \qquad (1)$$

where M = Li, Na, K, Rb, and Cs. In order to evaluate the relative stability between the left and right hand sides of reaction (1), the stabilization energy of the $M^+\bullet$18C6 complexes should be obtained. Experimentally, mass spectrometric, collision-induced dissociation and ion mobility studies have been applied to alkali metal ion–crown ether complexes by Armentrout, Dearden, Brodbelt, Bowers, and their co-workers.[6-29] These gas-phase studies for the non-solvated $M^+\bullet$18C6 complexes demonstrate that the intrinsic affinity of 18C6 is controlled primarily by the ion charge density. The binding energy of the $M^+\bullet$18C6 complexes thus ranges according to the ion size as $Li^+ > Na^+ > K^+ > Rb^+ > Cs^+$. This conclusion contradicts the observation of selective capturing of K^+ in the liquid phase and implies that solvent plays a crucial role in this selectivity.[10-12,21] Kollman and co-workers suggested from their molecular mechanics (MM) calculations that the selectivity of K^+ over Na^+ by 18C6 in aqueous solution is due to the fact that the difference in hydration energies of Na^+ and K^+ is larger than the

difference in stabilization energies of Na^+•18C6 and K^+•18C6.[30] Later, van Elden et al.[31] and Dang[32] drew a similar conclusion from their molecular dynamics (MD) studies. Accounting for microhydration of M^+ and M^+•18C6, reaction (1) can be written[4,5]

$$K^+\bullet 18C6 + M^+\bullet(H_2O)_m \rightleftharpoons M^+\bullet 18C6 + K^+\bullet(H_2O)_m \qquad (2)$$

$$K^+\bullet 18C6\bullet(H_2O)_n + M^+\bullet(H_2O)_m \rightleftharpoons M^+\bullet 18C6\bullet(H_2O)_n + K^+\bullet(H_2O)_m \qquad (3).$$

Armentrout and co-workers evaluated the enthalpy change of reaction (2) by using experimentally-determined enthalpies of M^+•18C6 and $M^+\bullet(H_2O)_m$, demonstrating that five and six H_2O molecules (m = 5 and 6) make the left hand side of reaction (2) more stable for all the alkali metal ions.[10,11] Glendening, Feller and Thompson reported *ab initio* studies of the complexes in reactions (2) and (3).[4,5] They extended their calculations to $M^+\bullet 18C6\bullet(H_2O)_n$ with n = 1–6 and obtained the enthalpy change of reactions (2) and (3) based on the calculated enthalpies. For reaction (2), only four H_2O molecules (m = 4) change the ion selectivity to $K^+ > Rb^+ \sim Na^+ > Cs^+ > Li^+$, the same as that measured in water. For reaction (3), the addition of up to six water molecules to the M^+•18C6 complexes drastically reduces the discrepancy between the measured and calculated enthalpy change for aqueous solutions. These experimental and theoretical studies both suggest that the net effects due to hydration of not only the M^+ ions, but also of the M^+•18C6 complexes are of great importance for determining the ion binding selectivity in solution. It was also pointed out that entropic effects, which were missing in the above studies, should be included to fully understand the ion selectivity, because the encapsulation process remains endothermic simply by considering only the enthalpy contribution.[5,10,11] In order to examine the entropic contribution, one has to determine the structure of the complexes related to equations

(1–3), which would allow a precise evaluation of vibrational frequencies; Glendening et al. mentioned that low-frequency vibrations must be obtained to better than 10 cm^{-1} to obtain kcal/mol accuracy for the entropy.[4] In addition, the number of conformers will also affect the ion selectivity; the larger the number of conformations a specific complex adopts, the more favorable is its formation. Apart from X-ray diffraction analysis in crystals, there are only a few reports that determine structures of the alkali metal ion–18C6 complexes and their hydrated species at the atomic level with conformational resolution. Average conformations of the M^+•18C6 complexes in the gas phase and in water have been determined from MM and MD studies.[30-38] The MD simulations in aqueous solution demonstrated that the Na^+ and K^+ ions are located at the center of mass of 18C6 in water, whereas the Rb^+ and Cs^+ ions are displaced from the center because of their larger size.[32-36] The K^+•18C6 simulation in water showed that on average two H_2O molecules are coordinated to K^+, one each from above and below the crown center.[35,36] *Ab initio* studies of the hydrated M^+•18C6 complexes also determined their stable conformations,[4,5] however since the main purpose of these *ab initio* studies was to obtain thermochemical values related to ion selectivity, the conformational search of the M^+•18C6•$(H_2O)_n$ complexes was not sufficiently extensive. Experimentally, Poonia determined the position of a H_2O molecule in the crystal of alkali metal halide–crown ether complexes using X-ray analysis and IR spectroscopy; an H_2O molecule was considered to be metal-coordinated on top of the K^+•18C6 complex.[39] Metal ion–crown ether complexes were also examined in water solutions by NMR, IR spectroscopy and some other techniques, but the hydration structure of the complexes remained unclear.[40,41] More recently, the structure of alkali metal ion–crown ether complexes has been investigated in the gas phase by both IR[42-45] and UV spectroscopy.[46-51] However, only Rodriguez, Vaden, and Lisy have reported IR

spectroscopy of *hydrated* M^+•18C6 complexes in the gas phase.[52-54] These studies attribute the observed IR spectra to multiple isomers, but the number of conformations and their relative contributions to the spectra are not clear because of broad and congested spectral features.[52-54] We have recently reported highly resolved UV and IR spectra of alkali metal complexes with dibenzo-18-crown-6 (DB18C6), benzo-18-crown-6 (B18C6) and benzo-15-crown-5 (B15C5) in a cooled, 22-pole ion trap.[49-51] These benzo-crown ethers have not been studied as extensively as 18C6, but one advantage of using them is that they have very sharp vibronic bands in UV absorption under cold conditions.[49-51] Resolved vibronic bands enable us to distinguish different conformers and measure conformer-specific IR spectra. We found that the alkali metal ion complexes of DB18C6 and B18C6 have structures similar to the corresponding 18C6 complexes, despite the structural constraints due to the benzene rings.[49-51]

In the present work, we investigate the conformations of cold complexes of DB18C6 with the potassium ion and water, K^+•DB18C6•$(H_2O)_n$ (n = 1–5). We employ IR-UV double resonance spectroscopy to measure conformer-selective infrared spectra of the cold species in the OH stretching (3200–3800 cm^{-1}) region. We determine the number and the structure of the conformers by comparing the observed IR spectra and those calculated by quantum chemical methods. Finally, we present the experimental and computational results for Rb^+•DB18C6•$(H_2O)_3$ and Cs^+•DB18C6•$(H_2O)_3$ complexes, demonstrating the uniqueness of the K^+•DB18C6 complex.

2. Experimental and computational methods

The details of our experimental approach have been given elsewhere.[49,55] Briefly, the K^+•DB18C6•$(H_2O)_n$ complexes are produced continuously at atmospheric pressure *via* nanoelectrospray of a solution containing potassium chloride and DB18C6 (~10 μM each) dissolved in methanol/water (~9:1 volume ratio). The parent ions of interest are mass-selected in a quadrupole mass filter and injected into a 22-pole RF ion trap, which is cooled by a closed cycle He refrigerator to 6 K. The trapped ions are cooled internally and translationally to ~10 K through collisions with cold He buffer gas,[49,55-57] which is pulsed into the trap. The trapped ions are then irradiated with a UV laser pulse, which causes some fraction of them to dissociate. The resulting charged photofragments, as well as the remaining parent ions, are released from the trap, mass-analyzed by a second quadrupole mass filter and detected with a channeltron electron multiplier. Ultraviolet photodissociation (UVPD) spectra of parent ions are obtained by plotting the yield of a particular photofragment ion as a function of the wavenumber of the UV laser. For IR-UV double resonance spectroscopy, the output pulse of an IR OPO precedes the UV pulse by ~100 ns and counter-propagates collinearly with it through the 22-pole. Absorption of the IR light by the ions in a specific conformational state warms them up, reducing the net UV absorption by the ions in this conformer.[58] The wavenumber of the UV laser is fixed to a vibronic transition of this conformer for monitoring the conformer-selective IR-induced depletion of the UVPD yield, and the wavenumber of the OPO is scanned in the OH stretching region (3200–3800 cm^{-1}) while monitoring the number of fragment ions. IR-UV depletion spectra are obtained by plotting the yield of a particular photofragment as a function of the OPO wavenumber.

For geometry optimization of the K^+•DB18C6•$(H_2O)_n$ complexes, we first use a classical force field to find conformational minima. The initial conformational search is performed by using the mixed torsional search with low-mode sampling and the AMBER* force field as implemented in MacroModel V. 9.1.[59] Minimum-energy conformers found with the force field calculations are then optimized at the M05-2X/6-31+G(d) level with *loose* optimization criteria using the GAUSSIAN09 program package.[60] The unique minima obtained by comparison of relative energies and rotational constants are further optimized using combinations of the M05-2X or ωB97XD functional and 6-31+G(d) or 6-311++G(d,p) basis set. Vibrational analysis is carried out for the optimized structures at the same computational levels. Calculated frequencies at the M05-2X/6-31+G(d) level are scaled with a factor of 0.9525 for comparison with the IR-UV spectra. The IR spectra of a specific conformer calculated at different levels are similar to each other (see Fig. 2S in the Supporting Information), whereas the relative stability of stable conformers depends on the employed level, especially for the n = 2 and 3 complexes. We therefore validate structures of the K^+•DB18C6•$(H_2O)_n$ complexes based on similarity of their observed and calculated IR spectra. All stable conformers are named systematically using "K1a" notation, where the first, capital letter indicates the metal ion of a complex, the subsequent number represents the number of the attached H_2O molecules, and the final lower case letter stands for the stability order of conformers determined at the M05-2X/6-31+G(d) level with (non-scaled) zero-point energy correction. All the conformers with a total energy less than 5 kJ/mol relative to that of the most stable structure are shown in Figs. 3S–7S of the Supporting Information.

3. Results

Figure 1 shows the UVPD spectra of the cooled K^+•DB18C6•$(H_2O)_n$ (n = 0–5) complexes. The spectra for $n > 0$ are measured by monitoring the yield of the bare K^+•DB18C6 photofragment ion. All the UVPD spectra in Fig. 1 show a number of vibronically resolved bands. The origin band of bare K^+•DB18C6 is observed at 36415 cm^{-1}.[49] All the K^+•DB18C6•$(H_2O)_n$ complexes show a red shift of the absorption relative to non-hydrated K^+•DB18C6. For the n = 1 complex, the origin band is found at 36274 cm^{-1}. The n = 2 complex has a strong UV band at 36326 cm^{-1}, and weak vibronic bands appear from 36267 cm^{-1}. In the UVPD spectra of n = 3 and 5, the origin band clearly appears at 36108 and 36154 cm^{-1}, respectively. For the n = 4 ion, the UVPD spectrum is more congested than those of other complexes. As shown by dotted lines in Figs. 1d and 1f, the UVPD spectra of the n = 3 and 5 complexes contain weak features that seem to correspond to the vibronic bands of the n = 2 and 4 complexes, respectively. These bands could appear in the UV spectra *via* the evaporation of one H_2O molecule from the mass-selected n = 3 or 5 complex due to metastable decay of hot complexes after the first quadrupole or induced by collisions with He buffer gas in the 22-pole, followed by cooling and UV excitation. In the n = 4 spectrum, however, we cannot find any band due to the fragment n = 3 complex. These results imply that the n = 4 complex will have a specific structure that is different from the n = 3 and 5 ions.

We measure the IR-UV spectra of the K^+•DB18C6•$(H_2O)_n$ complexes by fixing the UV wavenumber at the positions pointed by the arrows in Fig. 1 and scanning the wavenumber of the IR OPO. The IR-UV spectra recorded by fixing the UV frequency where there is no vibronic band provide IR gain spectra that are a sum of

different conformers, if they exist.[50] We first measure IR gain spectra at non-resonant UV frequencies to see the IR absorption of all the conformers and then measure IR dip spectra with the UV fixed on specific vibronic bands to attribute IR bands to each conformer. Figure 2a displays the IR-UV spectrum of the n = 1 complex in the OH stretching region measured by monitoring the intensity of the origin band at 36274 cm^{-1} in Fig. 1b as the IR laser wavenumber is scanned. Vibrational bands are observed at 3715 and 3615 cm^{-1}. Figures 2b and 2c show the calculated IR spectra of stable conformers (K1a and K1b) of the n = 1 complex; the structure of these conformers is illustrated in Fig. 3a and Fig. 3S. Since the calculated IR spectra of both K1a and K1b reproduce the observed IR bands well, one cannot determine the structure from the spectral comparison only. However, since K1a is more stable than K1b at all the calculation levels performed in this study by more than 2 kJ/mol, we attribute the structure of the n = 1 complex to K1a. The H_2O molecule in this structure is directly bound to the K^+ ion on top of K^+•DB18C6, and one OH group is H-bonded to one of the benzene rings. The vibrational analysis of K1a assigns the IR bands at 3715 and 3615 cm^{-1} to the anti-symmetric and symmetric OH stretching vibrations of H_2O, respectively. The positions of the vibronic bands at which the IR spectra are observed, the IR band positions and the conformer assignment are collected in Table 1.

Figures 4a–4c display the IR-UV spectra of the n = 2 ion measured with the UV laser fixed at 36226, 36326, and 36267 cm^{-1}, respectively. In the UVPD spectrum of the n = 2 complex (Fig. 1c), no band is seen below 36267 cm^{-1}. Thus, gain signals in the IR-UV spectrum measured at 36226 cm^{-1} (Fig. 4a) are due to IR absorption followed by UV absorption from vibrationally excited K^+•DB18C6•$(H_2O)_2$. The IR spectrum taken with the UV laser at 36226 cm^{-1} should thus contain IR bands of all conformers present in the ion trap. The IR spectrum taken with the UV set on the

sharp band at 36326 cm^{-1} shows depletion bands at 3452, 3601, and 3721 cm^{-1} and a weak bump at ~3710 cm^{-1}. These spectral features are similar to those of the gain spectrum in Fig. 4a. However, the IR-UV spectrum at 36267 cm^{-1} (Fig. 4c) provides different shapes from the IR spectrum at 36326 cm^{-1} (Fig. 4b); the IR spectrum in Fig. 4c shows gain and depletion signals around 3720 cm^{-1}. Since the vibronic band at 36267 cm^{-1} is quite weak, the conformer associated with this band is a minor one for the n = 2 complex. The IR spectrum measured with the UV at 36267 cm^{-1} is likely to be affected by the gain signal due to the absorption of the main conformer. Hence the gain signal around 3720 cm^{-1} in Fig. 4c is probably due to the main conformer associated with the strong UV band at 36326 cm^{-1}. In addition, there is a very small but noticeable difference in the position of the H-bonded OH stretch between the spectra in Figs. 4b and 4c (3452 and 3454 cm^{-1}, respectively). We thus conclude from the IR-UV results in Fig. 4 that there are at least two conformers that have very similar IR spectra. Figures 4d–4j illustrate the IR spectra calculated for stable conformers of n = 2 (K2a–K2g), the structures of which are shown in Fig. 3 and Fig. 4S. Among these conformers, K2d and K2f (Figs. 4g and 4i) have a strong band around 3450 cm^{-1}, similar to the IR-UV spectra. In both of these conformers the two H_2O molecules form a chain structure, with one of them having a direct intermolecular bond with the K^+ ion. Similar to the case of the n = 1 ion, K2d, which has the H_2O molecules bound on top of DB18C6, is more stable than K2f at all the calculation levels performed in this study. Hence we attribute the main conformer having the strong UV band at 36326 cm^{-1} to K2d and the weak vibronic band at 36267 cm^{-1} to K2f.

The observed and calculated IR spectra of the n = 3 complex are displayed in Fig. 5. The stable conformers are shown in Fig. 6 and Fig. 5S. The IR-UV spectrum measured at a non-resonant UV position (36076 cm^{-1}, Fig. 5a) shows more gain bands

than the number of the OH groups of the complex, suggesting the existence of multiple conformers. These IR-UV bands are attributed to three spectra, as seen in Figs. 5b–5d. Figure 5b shows the IR-UV spectrum measured at the strongest UV band at 36108 cm^{-1}. This is similar to the calculated IR spectrum of K3a (Fig. 5e), which is the most stable conformer of the $n = 3$ ion. Therefore, the UV band at 36108 cm^{-1} can be assigned to K3a. In K3a (Fig. 6a), two H_2O molecules are directly bound to the K^+ ion and donate one OH group to the other H_2O. All the H_2O molecules are located on top of one phenyl ring of the DB18C6. The IR-UV spectra measured at 36326 and 36390 cm^{-1} (Figs. 5c and 5d) have a strong IR band below 3500 cm^{-1}. In analogy with the $n = 2$ spectra, these IR bands can be ascribed to the H-bonded OH stretch of H_2O forming a water chain. The IR-UV spectrum at 36326 cm^{-1} (Fig. 5c) shows the H-bonded OH stretch at 3452 cm^{-1}, which is the same as that of the $n = 2$ conformer at 36326 cm^{-1} (Fig. 4b). This UV position in the $n = 3$ spectrum (36326 cm^{-1}) coincides with that of the main conformer of $n = 2$ (see Figs. 1c and 1d). Therefore, the 36326 cm^{-1} band in the UV spectrum of the $n = 3$ ion and the IR-UV spectrum measured at this UV position (Fig. 5c) can be attributed to the $n = 2$ complex produced by one H_2O vaporization from the mass-selected $n = 3$ complex between the first quadrupole and the 22-pole ion trap. Since no band is seen at 36390 cm^{-1} in the $n = 2$ spectrum, the 36390 cm^{-1} band in the UVPD spectrum of the $n = 3$ ion is ascribed to the intact $n = 3$ complex. Among the stable conformers of $n = 3$, K3d and K3g (Figs. 6b and 5S) have H_2O chain forms. The 3602 cm^{-1} band in Fig. 5d is well reproduced by the ~3593 cm^{-1} band of K3g. Hence, the UV band of the $n = 3$ complex at 36390 cm^{-1} is assigned to K3g. Conformer K3g has two H_2O molecules on the top and one at the bottom.

The IR-UV and calculated IR spectra of the $n = 4$ and 5 complexes are displayed in Figs. 7 and 8. The stable conformers are shown in Figs. 9, 6S, and 7S.

There are only two and four conformers calculated below 5 kJ/mol for the n = 4 and 5 complexes, respectively. The IR gain spectra measured at non-resonant UV positions (Figs. 7a and 8a) are quite similar to the depletion spectra at strong UV bands (Figs. 7b and 8b), suggesting that the n = 4 and 5 complexes have only one stable conformer each. The IR-UV spectra are well reproduced by the IR spectra calculated for the most stable conformers (K4a and K5a in Fig. 9). We thus attribute the structure of the n = 4 and 5 complexes to K4a and K5a, respectively. In isomer K4a, four H_2O molecules form one ring, which is symmetrically attached on top of the K^+ ion. Also in K5a, a five-membered ring is constructed and bound to the K^+ ion and one of the oxygen atoms of DB18C6 *via* the H-bond.

4. Discussion

The K^+•DB18C6 complex has a boat-type C_{2v} conformer in the gas phase,[49] which is different from the symmetric D_{3d} conformation of the K^+•18C6 complex. This bent structure of K^+•DB18C6, which is due to structural constraints by the two benzene rings, affects the manner in which it is hydrated. In the case of the n = 1 complex, two types of conformers (K1a and K1b) are predicted by the calculations to be stable, with the H_2O molecule bound on top in the former and on the bottom in the latter (Figs. 3 and 3S). Conformer K1a is more stable than K1b at all levels of calculation performed in this study. Figure 10a displays the distance between the metal ions and the oxygen mean plane of DB18C6 in the K^+•DB18C6•$(H_2O)_n$, Rb^+•DB18C6•$(H_2O)_n$, and Cs^+•DB18C6•$(H_2O)_n$ complexes. The attachment of one H_2O molecule on the top in K1a enlarges this distance from 0.51 (n = 0) to 0.72 Å. In contrast, K1b has a shorter distance (0.13 Å, not shown in Fig. 10a) than that of the n = 0 complex.

However, the $K^+ \bullet\bullet\bullet O_{water}$ distance is almost the same for K1a (2.72 Å) and K1b (2.71 Å). It therefore seems that both K1a and K1b are stabilized by optimizing the distance between K^+ and H_2O at the expense of the interaction between K^+ and DB18C6. Figure 10b displays the potential energy curve of the K^+•DB18C6 complex as a function of the distance between the K^+ ion and the oxygen mean plane of DB18C6; the energy of K^+•DB18C6 is calculated at the M05-2X/6-31+G(d) level, freezing the conformation of the DB18C6 part. The potential curve has a minimum around 0.5 Å, which corresponds to the stable form of the K^+•DB18C6 complex. From this potential, the difference in the energy at 0.72 Å (K1a) and 0.13 Å (K1b) is estimated to be 1.43 kJ/mol, which indicates that the K^+•DB18C6 component in K1a is 1.43 kJ/mol more stable than that in K1b. We thus attribute the larger stability of K1a over K1b principally to the stability of the K^+•DB18C6 component in these conformers. The energy difference between K1a and K1b is calculated to be 2.60 kJ/mol (see Fig. 3S), which is larger than 1.43 kJ/mol estimated from the displacement of the metal ion relative to the crown ether. This is probably due to the interaction between H_2O and one of the benzene rings in K1a (Fig. 3a). A similar argument can reasonably explain the relative stability of conformers K2d and K2f of the n = 2 complex; K2d is more stable than K2f at all levels of calculation. These conformers have a chain of H_2O molecules, and the $K^+ \bullet\bullet\bullet O_{water}$ distance of K2d (2.65 Å) is comparable to that of K2f (2.69 Å). Therefore, the major difference in the structure between K2d and K2f is the hydration site, similar to the difference between K1a and K1b. As shown in Fig. 10a, K2d and K2f have $K^+ \bullet\bullet\bullet$(oxygen mean plane of DB18C6) distances of 0.72 and 0.15 Å, respectively. According to the potential curve in Fig. 10b, the difference in the energy at 0.72 and 0.15 Å is estimated to be 1.19 kJ/mol. This is almost the same as the difference in the total energy between K2d and K2f (~1.2 kJ/mol, see Fig. 4S). The

preference of K2d over K2f thus seems to originate from its more favorable conformation of the K^+•DB18C6 part of the complex.

As mentioned above, the spectra of the $n = 3$ complex indicate the presence of two stable conformers in the ion trap. This is characteristic of the K^+ complex compared to the Rb^+ and Cs^+ complexes. The measured and calculated IR spectra of the Rb^+•DB18C6•$(H_2O)_3$ and Cs^+•DB18C6•$(H_2O)_3$ complexes are shown in Fig. 11. (The UVPD spectra of these complexes are displayed in the Supporting Information, Fig. 1S.) The IR-UV gain spectra in Figs. 11a and 11d, which are measured at non-resonant UV positions, are similar to the IR-UV depletion spectra monitored at strong vibronic bands (Figs. 11b and 11e). This indicates that there is only one conformer for each of the Rb^+•DB18C6•$(H_2O)_3$ and Cs^+•DB18C6•$(H_2O)_3$ complexes. The structures of the Rb^+•DB18C6•$(H_2O)_3$ and Cs^+•DB18C6•$(H_2O)_3$ complexes are attributed to the most stable isomers, Rb3a and Cs3a, respectively, on the basis of the similarity between the IR-UV spectra and the calculated IR spectra, as shown in Fig. 11. Both conformers Rb3a and Cs3a strongly resemble conformer K3a of the K^+•DB18C6•$(H_2O)_3$ complex (Fig. 6a). The high stability of K3a, Rb3a, and Cs3a can be ascribed to the displaced position of the metal ions in the M^+•DB18C6 complexes. The metal ions in the non-hydrated K^+•DB18C6, Rb^+•DB18C6, and Cs^+•DB18C6 complexes deviate from the oxygen mean plane of DB18C6 by 0.51, 1.00, and 1.36 Å, respectively.[49,50] Therefore, it is quite probable that the H_2O molecules in the M^+•DB18C6•$(H_2O)_3$ complexes tend to stay above the M^+ ion to have direct intermolecular bonds with the metal ions. On the other hand, another conformer (K3g) coexists for the K^+•DB18C6•$(H_2O)_3$ complex. This is likely due to the optimum matching between the K^+ ion and the crown cavity. Compared to Rb^+ and Cs^+ ions, the K^+ ion is effectively encapsulated by DB18C6, making the interaction between K^+ and

H_2O molecules weak. As a result, different modes of hydration such as in K3a and K3g can occur for the K^+•DB18C6 complex. Multiple conformations for the K^+•DB18C6•$(H_2O)_3$ complex imply an advantage for the effective capture of the K^+ ion by DB18C6 over the Rb^+ and Cs^+ ions in water; the more conformations the complex takes, the more favorable the complex formation becomes. In contrast, one conformer is predominantly stable for the larger K^+•DB18C6•$(H_2O)_n$ (n = 4 and 5) complexes. In these complexes, the H_2O molecules are bound to the K^+ ion cooperatively by forming an H_2O ring, and the K^+ ion is pulled out from the DB18C6 cavity more than the smaller complexes. In particular, the n = 4 complex has a quite symmetric structure (K4a in Fig. 9a); the ring with four H_2O molecules looks the most suitable for the solvation to the K^+•DB18C6 complex.

Finally, we are left with one problem unsolved: the disagreement between the conformers found in the experiment and the order of the conformer stability obtained in the quantum chemical calculations for the n = 2 and 3 complexes. Since the IR spectra provide quite distinguishable signatures for the conformation, the determination of the complex structure based on the IR spectra should be reliable. Hence, the discrepancy originates either from the deficiency of the calculations or from the conformer formation mechanism, specific to our experiment. To resolve this we first tried further conformational search using a different (MMFFs) force field,[59] however, we obtain only similar conformers as those in the AMBER* calculations. In addition, we calculated the total energy of the complexes at the M05-2X/6-311++G(d,p), ωB97XD/6-31+G(d), ωB97XD/6-311++G(d,p), and MP2/6-31+G(d) levels. The relative total energy is dependent on the calculation methods, but the order of the stability does not change drastically. This leads us to believe that the disagreement may be linked to the

formation process of the complexes in our experiment. One useful clue in support of this conclusion is hidden in the results of the $n = 2$ complex. In the calculations of the $n = 2$ complexes, the conformers in which the two H_2O molecules are independently bound to the K^+•DB18C6 component (K2a, K2b, and K2c, Fig. 4S) are predicted to be more stable than K2d and K2f, which are those we seem to observe in the experiment. Since K2d and K2f have an H_2O•••H_2O intermolecular bond, it is probable that conformers that have H_2O•••H_2O intermolecular bonds can survive in the complex production. In the course of the formation of the hydrated complexes, charged liquid droplets from the nanoelectrospray experience numerous collisions with the drying gas used in the ion source or the atmosphere, promoting sequential evaporation of H_2O molecules. As seen in Fig. 9, the $n = 4$ and 5 complexes have a ring of H_2O molecules. When the next evaporation process occurs from K4a, a further cyclic closing with three H_2O molecules like the one in K3b or K3c (Fig. 5S) does not occur. Instead, the rearrangement of the H_2O molecules leads to the conformations like K3a (Fig. 6). It is reasonable that conformers K2d (Fig. 3b) and K1a (Fig. 3a) are produced by further evaporation from K3a. These formation processes described above are similar to the ones of the K^+•18C6•$(H_2O)_n$ complexes in the gas phase *via* K^+ impact with 18C6–water clusters followed by water evaporation.[53] In the 22-pole ion trap, the produced complexes collide with buffer He gas many times, but these collisions do not seem to induce the conformational isomerization. While the formation scheme of K2f and K3g is not clear, these conformers may be produced by the simultaneous evaporation of water clusters from relatively larger complexes. However, since the UV bands assigned to K2f (36267 cm^{-1} in Fig. 1c) and K3g (36390 cm^{-1} in Fig. 1d) are weaker than the main vibronic bands, simultaneous evaporation is thought to be a minor process.

For the K^+•DB18C6•$(H_2O)_n$ complexes, the conformers that have all the H_2O molecules on top of the K^+•DB18C6 complex appear to be more favorable. In contrast, the MD simulations of the K^+•18C6 complex in water suggested that the K^+ ion is coordinated by one H_2O molecule each from the top and bottom sides of the K^+•18C6 complex on average.[35,36] Other MD simulations of the same system show that K^+ ion in the K^+•18C6 complexes are located at the center of mass of 18C6 in water, indicating symmetric hydration.[32-36] The "asymmetric" hydration in the K^+•DB18C6•$(H_2O)_n$ complexes such as K2d, K3a, K4a, and K5a is due to intrinsic stability of the boat form for the K^+•DB18C6 component. However, this asymmetric hydration is found also for the gas-phase K^+•18C6•$(H_2O)_n$ complexes.[53,54] In addition, the existence of conformers K2f and K3g, which have H_2O molecule(s) also at the bottom, implies that hydration on the bottom side of the K^+•DB18C6 component occurs in larger complexes. In order to shed further light on the effects of hydration on the K^+•DB18C6 encapsulation complexes, further examination of larger hydrated complexes will be indispensable.

5. Summary

We have previously reported the structures of the M^+•DB18C6 and DB18C6•$(H_2O)_n$ complexes in the gas phase under cold conditions.[49-51,61,62] This spectroscopic study is a final step towards developing a more complete understanding of the ion selectivity of host species in solution, following a number of previous gas-phase studies. We have measured UV photodissociation (UVPD) and IR-UV double resonance spectra of the K^+•DB18C6•$(H_2O)_n$ (n = 1–5) complexes produced by nanoelectrospray and cooled to ~10 K in a 22-pole ion trap. We have determined the number and the structure of the conformers of K^+•DB18C6•$(H_2O)_n$ with the aid of

quantum chemical calculations. Two kinds of intermolecular interaction control the structure of the hydrated complexes: the optimum matching in size between K^+ and DB18C6, and the cooperative effect of H_2O molecules. In the n = 2 and 3 ions, there are at least two conformers each, even under the cold conditions of our ion trap. Since the crown cavity can effectively shield the K^+ ion, the hydrated complexes do not adopt one predominant hydration form, providing multiple conformations. In contrast, cooperative hydration of the K^+ ion gives only one stable conformer each for the n = 4 and 5 complexes. At present, it is difficult to predict the structure of the K^+•DB18C6 complex in water or the main factor that controls the ion selectivity in solution only from the results of this study, because two possible factors (the optimum matching in size and cooperative effects of water molecules) seem to play a role even in the n = 2–5 complexes. However, multiple conformations observed for the K^+ complexes will have an advantage for the effective capture of the K^+ ion because of entropic effects. Previous mass spectrometric studies did not provide information on the number of conformers in the gas phase. In this study, the cooling of the complexes provides resolved UV transitions, which enable us determine the number of the conformers and measure conformer-specific IR spectra at the same time. Investigating larger gas-phase complexes with our method will provide further insight into the factor of the ion selectivity.

Acknowledgment

This work is partly supported by JSPS KAKENHI Grant Number 21350016, and the Swiss National Science foundation through grant 200020_130579 and École Polytechnique Fédérale de Lausanne (EPFL). YI and TE thank the support from JSPS

through the program “Strategic Young Researcher Overseas Visits Program for Accelerating Brain Circulation”.

Supporting Information Available: Results of the UVPD spectra of Rb^+•DB18C6•$(H_2O)_3$ and Cs^+•DB18C6•$(H_2O)_3$, all the stable structure of the K^+•DB18C6•$(H_2O)_n$ (n = 1–5) complexes, and a full list of authors of Ref. 60. This material is available free of charge *via* the internet at http://pubs.acs.org.

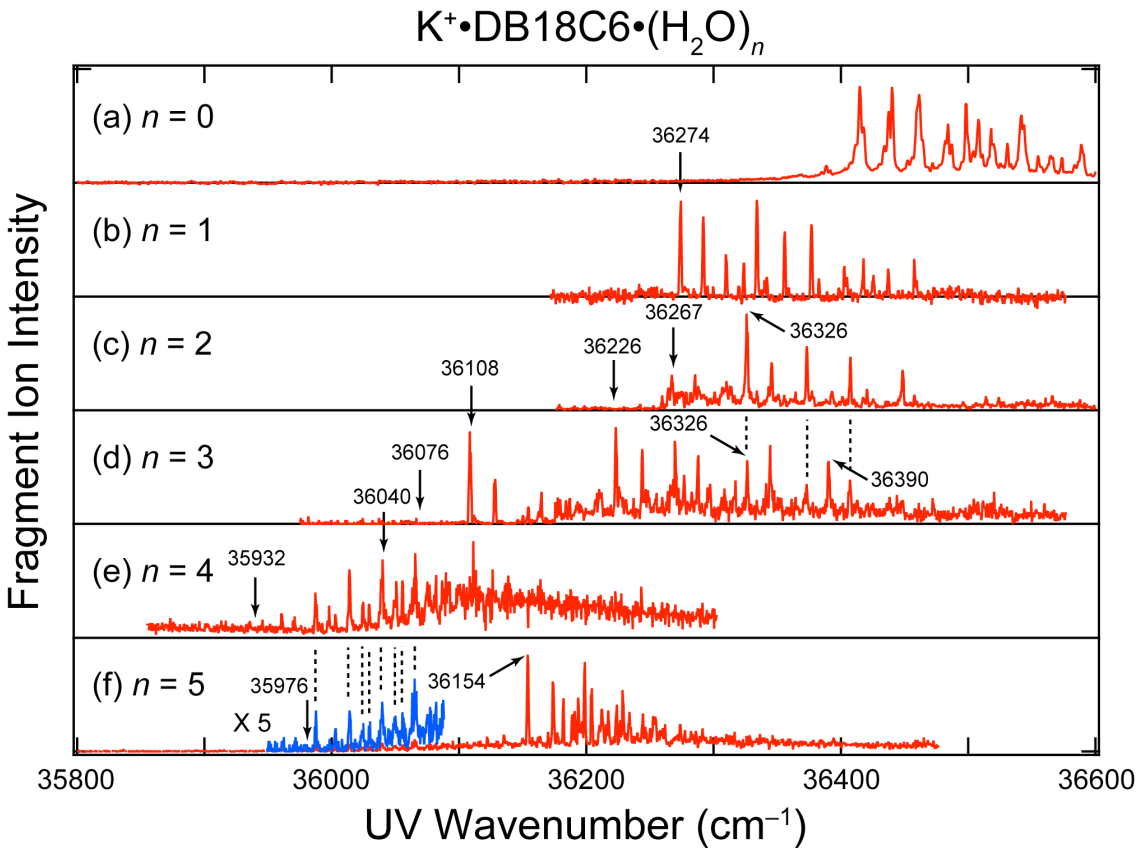

Figure 1. The UVPD spectra of the K^+•DB18C6•$(H_2O)_n$ (n = 1–5) complexes with that of bare K^+•DB18C6 complex (Ref. 49). The arrows show the UV positions at which the IR-UV spectra are measured.

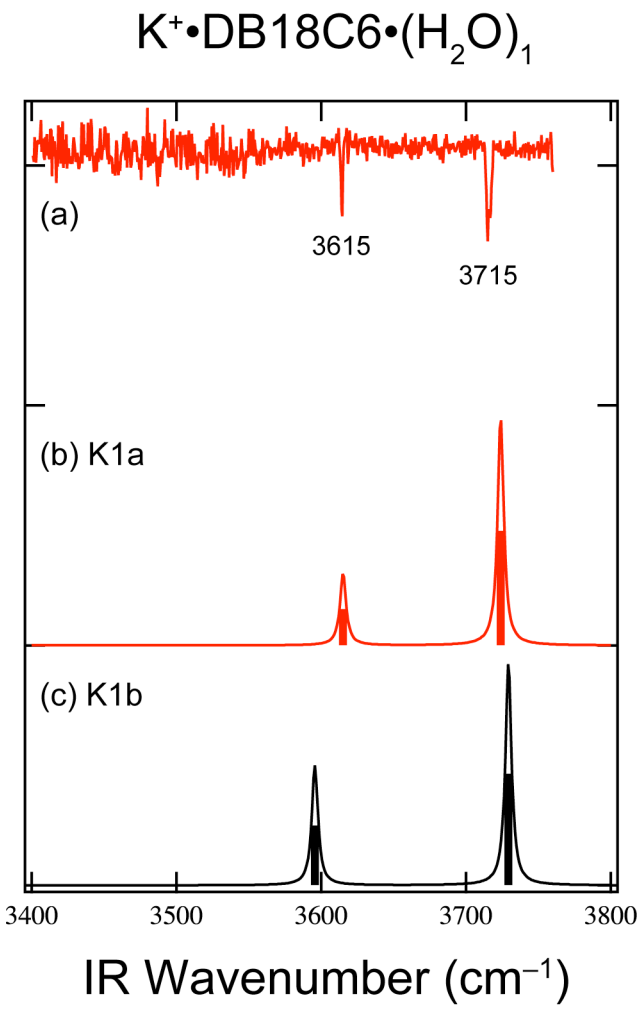

Figure 2. (a) The IR-UV spectrum of the K^+•DB18C6•$(H_2O)_1$ complex measured at the UV wavenumber of 36274 cm^{-1} (as shown with an arrow in Fig. 1b). (b, c) The IR spectra calculated for stable conformers (K1a and K1b). A scaling factor of 0.9525 is employed for the calculated vibrational frequencies.

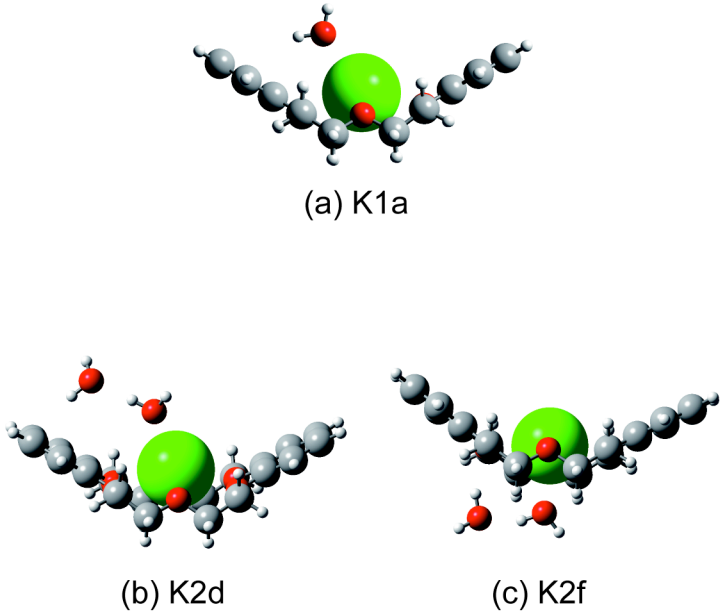

Figure 3. The structure of the n = 1 and 2 complexes determined by the comparison of the IR spectra observed and calculated.

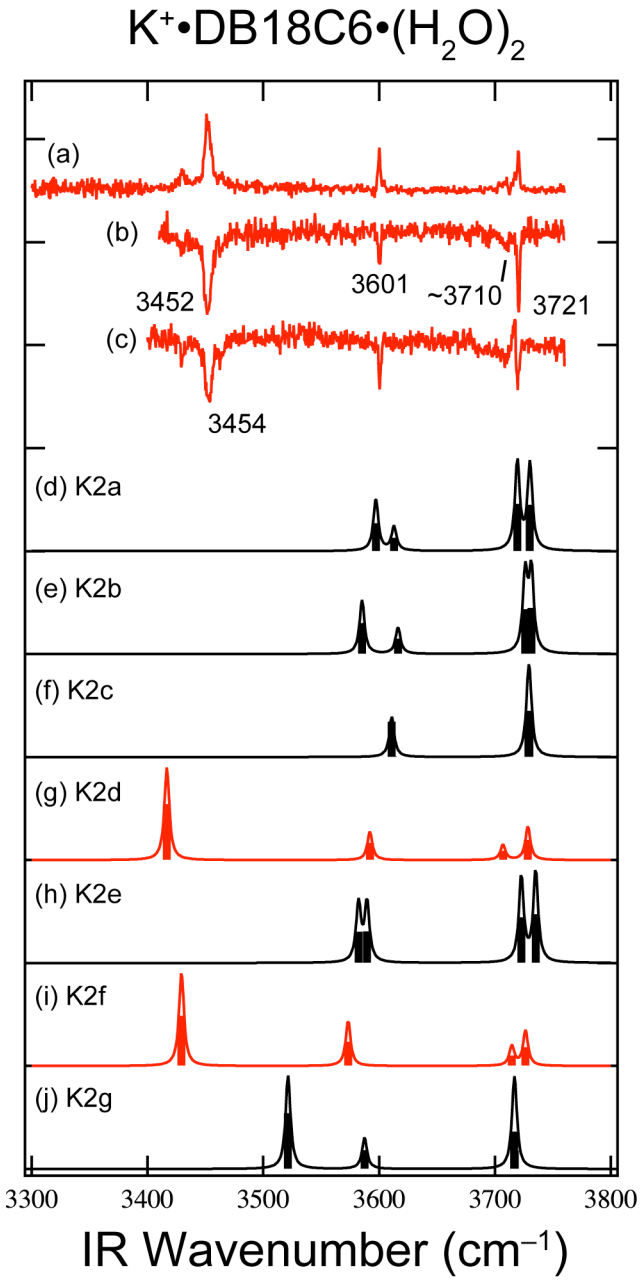

Figure 4. (a–c) The IR-UV spectra of the K^+•DB18C6•$(H_2O)_2$ complex measured at the UV wavenumbers of 36226, 36326, and 36267 cm^{-1}. The UV positions are shown with arrows in Fig. 1c. (d–j) The IR spectra calculated for stable conformers (K2a–K2g). A scaling factor of 0.9525 is employed for the vibrational frequencies calculated.

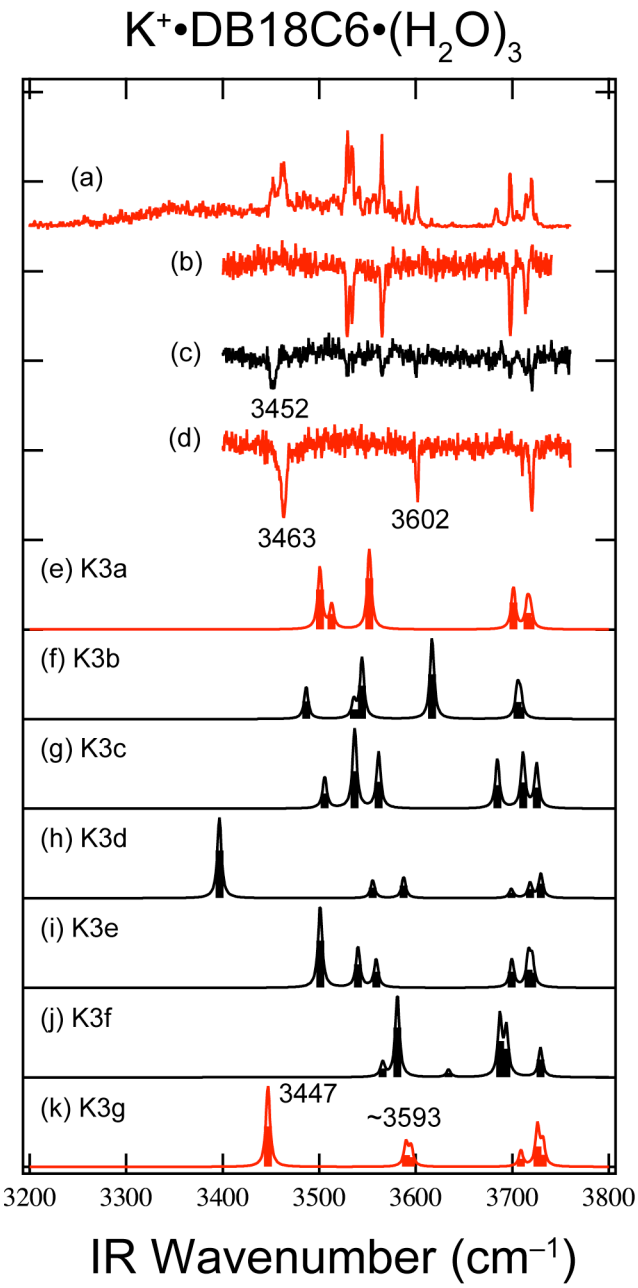

Figure 5. (a–d) The IR-UV spectra of the K^+•DB18C6•$(H_2O)_3$ complex measured at the UV wavenumbers of 36076, 36108, 36326, and 36390 cm^{-1}. The UV positions at which the IR-UV spectra are measured are shown with arrows in Fig. 1d. (e–k) The IR spectra calculated for stable conformers (K3a–K3g). A scaling factor of 0.9525 is employed for the vibrational frequencies calculated.

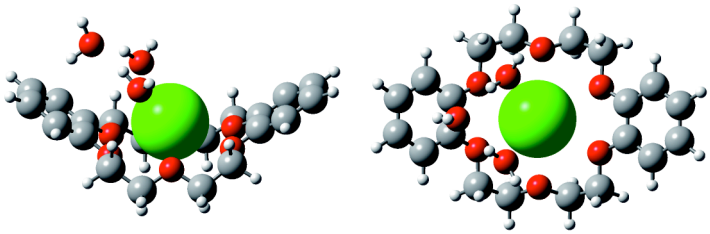

(a) K3a

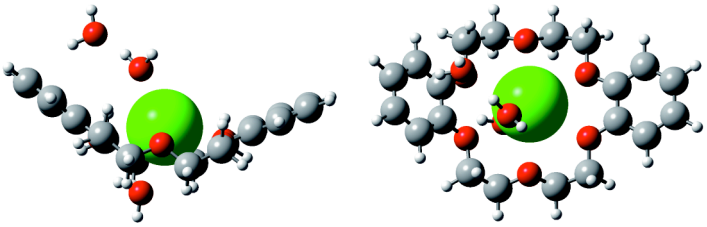

(b) K3g

Figure 6. Side and top views of the n = 3 complex determined by the comparison of the IR spectra observed and calculated.

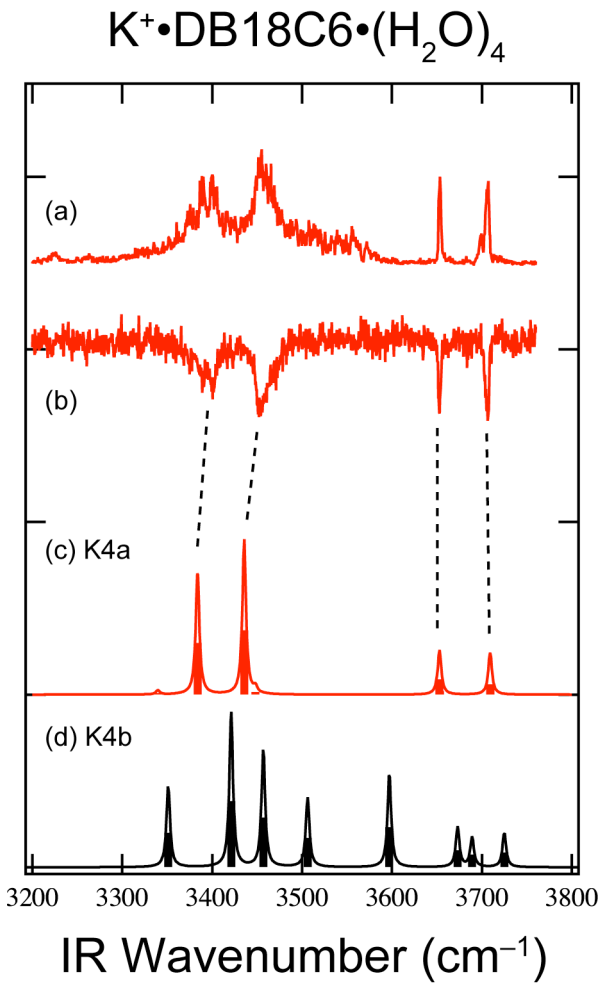

Figure 7. (a, b) The IR-UV spectra of the K^+•DB18C6•$(H_2O)_4$ complex measured at the UV wavenumbers of 35932 and 36040 cm^{-1}. The UV positions are shown with arrows in Fig. 1e. (c, d) The IR spectra calculated for stable conformers (K4a and K4b). A scaling factor of 0.9525 is employed for the vibrational frequencies calculated.

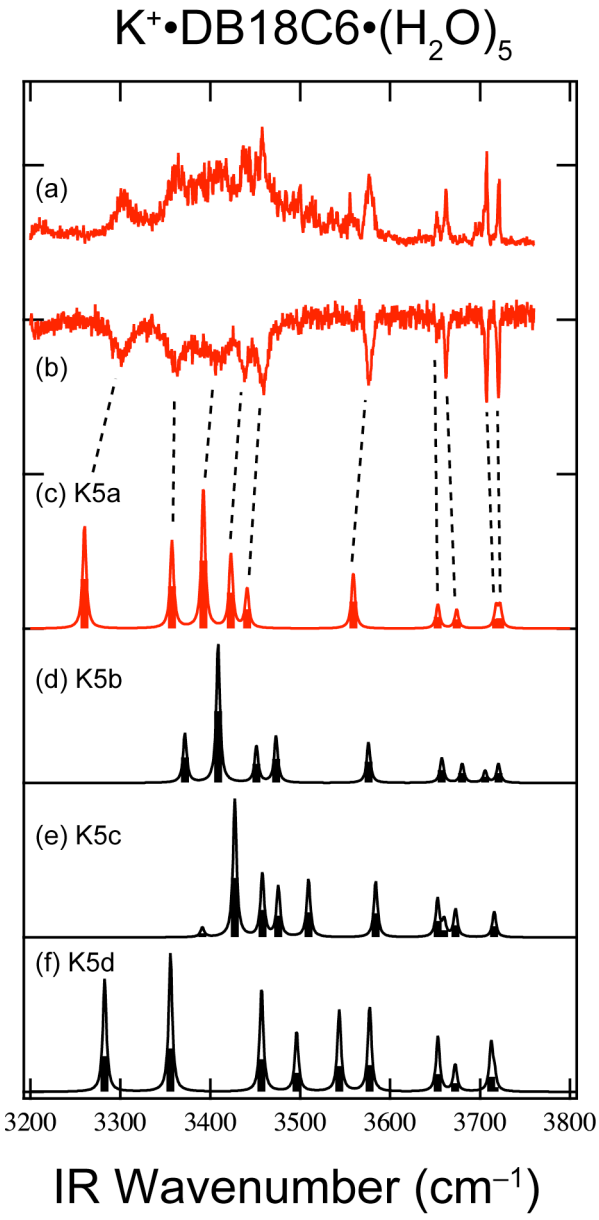

Figure 8. (a, b) The IR-UV spectra of the K^+•DB18C6•$(H_2O)_5$ complex measured at the UV wavenumbers of 35976 and 36154 cm^{-1}. The UV positions are shown with arrows in Fig. 1f. (c–f) The IR spectra calculated for stable conformers (K5a–K5d). A scaling factor of 0.9525 is employed for the vibrational frequencies calculated.

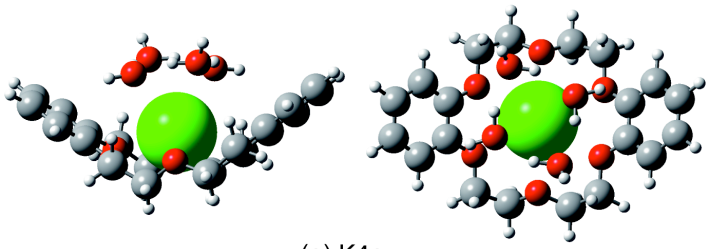

(a) K4a

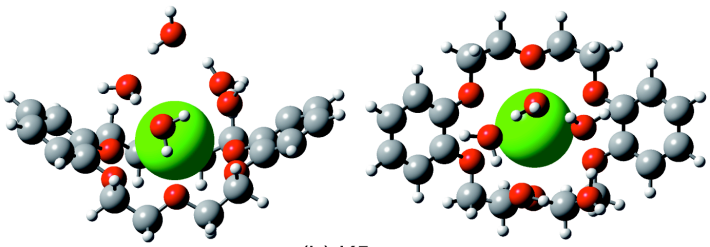

(b) K5a

Figure 9. Side and top views of the n = 4 and 5 complexes determined by the comparison of the IR spectra observed and calculated.

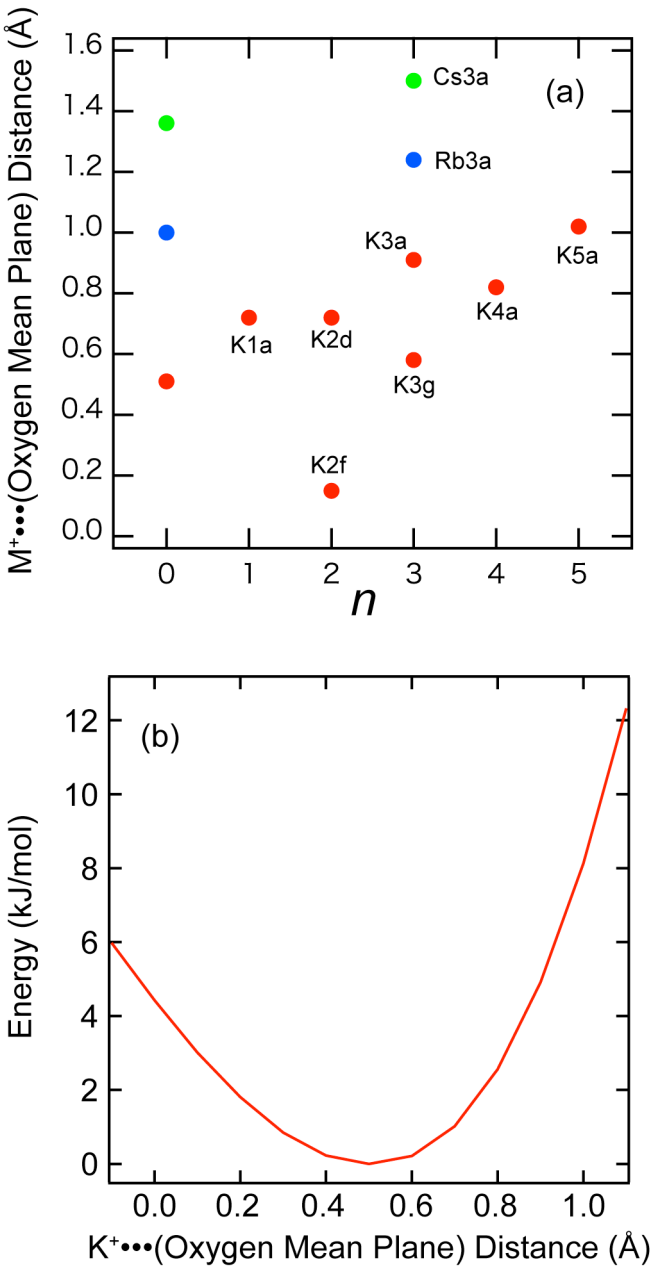

Figure 10. (a) Distance between the metal ion and the mean plane of the oxygen atoms of DB18C6 for the optimized structures of K^+•DB18C6•$(H_2O)_n$ (n = 0–5), Rb^+•DB18C6•$(H_2O)_n$ (n = 0, 3), and Cs^+•DB18C6•$(H_2O)_n$ (n = 0, 3). The values of the n = 0 complexes are taken from Ref. 50. (b) The potential energy curve of the K^+•DB18C6 complex as a function of the distance between the K^+ ion and the mean plane of the oxygen atoms of DB18C6 calculated at the M05-2X/6-31+G(d) level. In the calculations, the structure of the DB18C6 part is frozen.

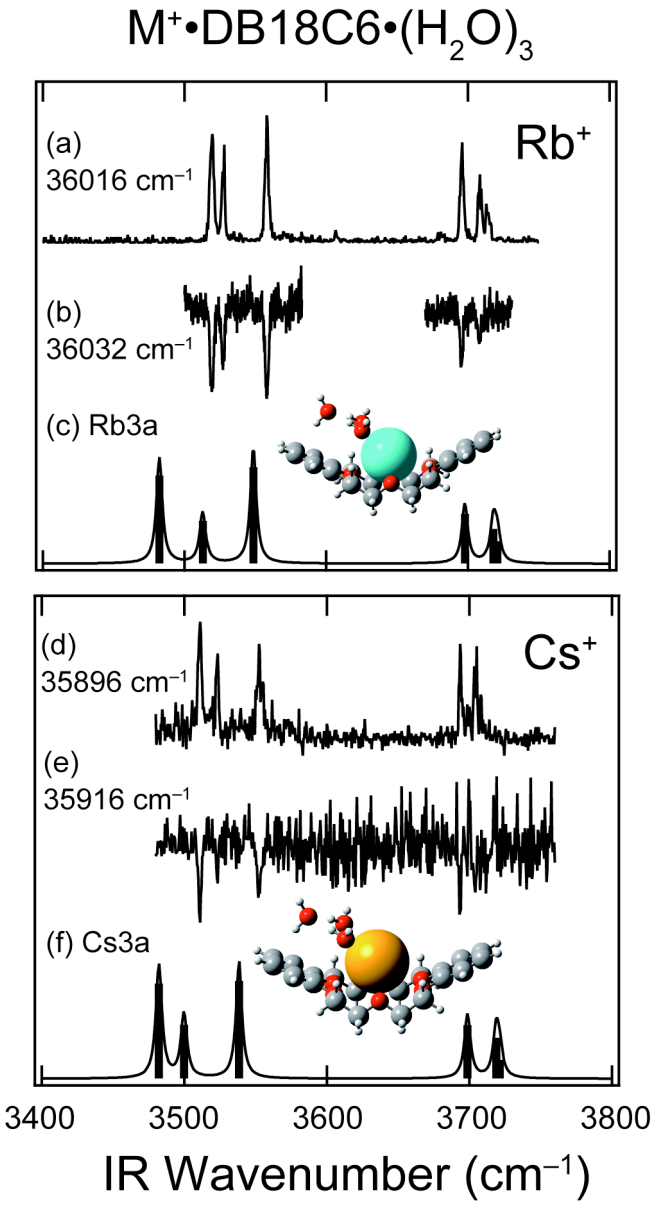

Figure 11. The IR-UV spectra of the Rb^+•DB18C6•$(H_2O)_3$ (a and b) and Cs^+•DB18C6•$(H_2O)_3$ (d and e) complexes. The UV positions at which the IR-UV spectra are measured are shown with arrows in Fig. 1S. (c and f) The IR spectra calculated for the most stable conformers (Rb3a and Cs3a). A scaling factor of 0.9525 is employed for the vibrational frequencies calculated.

Table 1. Positions of the UV bands (cm^{-1}) at which the IR-UV spectra have been measured, positions of the IR-UV bands (cm^{-1}), and conformation assignment of the K^+•DB18C6•$(H_2O)_n$ complexes.

n	UV Band Positions	IR Band Positions	Conformer
1	36274	3615, 3715	K1a
2	36326	3452, 3601, ~3710, 3721	K2d
	36267	3454, 3601, ~3720	K2f
3	36108	3529, 3534, 3565, 3698, 3714	K3a
	(36326)[a]	(3452)	(K2d)
	36390	3463, 3602, 3711, 3720	K3g
4	36040	~3400, ~3452, 3653, 3707	K4a
5	36154	~3301, ~3364, ~3412, ~3438, ~3460, 3576, 3652, 3662, 3708, 3721	K5a

[a]This band originates from the $n = 2$ complex produced via evaporation of one H_2O molecule from the mass-selected $n = 3$ ion between the first quadrupole and the 22-pole.

References

(1) Izatt, R. M.; Bradshaw, J. S.; Nielsen, S. A.; Lamb, J. D.; Christensen, J. J. *Chem. Rev.* **1985**, *85*, 271-339.

(2) Izatt, R. M.; Terry, R. E.; Haymore, B. L.; Hansen, L. D.; Dalley, N. K.; Avondet, A. G.; Christensen, J. J. *J. Am. Chem. Soc.* **1976**, *98*, 7620-7626.

(3) Allen, F. H. *Acta Crystallogr. B Struct. Commun.* **2002**, *58*, 380-388.

(4) Glendening, E. D.; Feller, D.; Thompson, M. A. *J. Am. Chem. Soc.* **1994**, *116*, 10657-10669.

(5) Feller, D. *J. Phys. Chem. A* **1997**, *101*, 2723-2731.

(6) Ray, D.; Feller, D.; More, M. B.; Glendening, E. D.; Armentrout, P. B. *J. Phys. Chem.* **1996**, *100*, 16116-16125.

(7) More, M. B.; Ray, D.; Armentrout, P. B. *J. Phys. Chem. A* **1997**, *101*, 831-839.

(8) More, M. B.; Ray, D.; Armentrout, P. B. *J. Phys. Chem. A* **1997**, *101*, 4254-4262.

(9) More, M. B.; Ray, D.; Armentrout, P. B. *J. Phys. Chem. A* **1997**, *101*, 7007-7017.

(10) More, M. B.; Ray, D.; Armentrout, P. B. *J. Am. Chem. Soc.* **1998**, *121*, 417-423.

(11) Armentrout, P. B. *Int. J. Mass Spectrom.* **1999**, *193*, 227-240.

(12) Armentrout, P. B.; Austin, C. A.; Rodgers, M. T. *Int. J. Mass Spectrom.* **2012**, *330*, 16-26.

(13) Zhang, H.; Chu, J. H.; Leming, S.; Dearden, D. V. *J. Am. Chem. Soc.* **1991**, *113*, 7415-7417.

(14) Zhang, H.; Dearden, D. V. *J. Am. Chem. Soc.* **1992**, *114*, 2754-2755.

(15) Chu, I. H.; Zhang, H.; Dearden, D. V. *J. Am. Chem. Soc.* **1993**, *115*, 5736-5744.

(16) Dearden, D. V.; Liang, Y. J.; Nicoll, J. B.; Kellersberger, K. A. *J. Mass Spectrom.* **2001**, *36*, 989-997.

(17) Anderson, J. D.; Paulsen, E. S.; Dearden, D. V. *Int. J. Mass Spectrom.* **2003**, *227*, 63-76.

(18) Maleknia, S.; Brodbelt, J. *J. Am. Chem. Soc.* **1992**, *114*, 4295-4298.

(19) Brodbelt, J. S. *Int. J. Mass Spectrom.* **2000**, *200*, 57-69.

(20) Kempen, E. C.; Brodbelt, J. S. *Anal. Chem.* **2000**, *72*, 5411-5416.

(21) Lee, S.; Wyttenbach, T.; Vonhelden, G.; Bowers, M. T. *J. Am. Chem. Soc.* **1995**, *117*, 10159-10160.

(22) Franski, R. *Rapid Commun. Mass Spectrom.* **2009**, *23*, 3488-3491.

(23) Franski, R. *Rapid Commun. Mass Spectrom.* **2011**, *25*, 672-674.

(24) Katritzky, A. R.; Malhotra, N.; Ramanathan, R.; Kemerait, R. C.; Zimmerman, J. A.; Eyler, J. R. *Rapid Commun. Mass Spectrom.* **1992**, *6*, 25-27.

(25) Leize, E.; Jaffrezic, A.; VanDorsselaer, A. *J. Mass Spectrom.* **1996**, *31*, 537-544.

(26) Malhotra, N.; Roepstorff, P.; Hansen, T. K.; Becher, J. *J. Am. Chem. Soc.* **1990**, *112*, 3709-3710.

(27) Peiris, D. M.; Yang, Y. J.; Ramanathan, R.; Williams, K. R.; Watson, C. H.; Eyler, J. R. *Int. J. Mass Spectrom. Ion Process.* **1996**, *157*, 365-378.
(28) Schalley, C. A. *Int. J. Mass Spectrom.* **2000**, *194*, 11-39.
(29) Schalley, C. A. *Mass Spectrom. Rev.* **2001**, *20*, 253-309.
(30) Wipff, G.; Weiner, P.; Kollman, P. *J. Am. Chem. Soc.* **1982**, *104*, 3249-3258.
(31) Van Eerden, J.; Harkema, S.; Feil, D. *J. Phys. Chem.* **1988**, *92*, 5076-5079.
(32) Dang, L. X. *J. Am. Chem. Soc.* **1995**, *117*, 6954-6960.
(33) Dang, L. X.; Kollman, P. A. *J. Am. Chem. Soc.* **1990**, *112*, 5716-5720.
(34) Dang, L. X. *Chem. Phys. Lett.* **1994**, *227*, 211-214.
(35) Dang, L. X.; Kollman, P. A. *J. Phys. Chem.* **1995**, *99*, 55-58.
(36) Thompson, M. A.; Glendening, E. D.; Feller, D. *J Phys. Chem.* **1994**, *98*, 10465-10476.
(37) Zwier, M. C.; Kaus, J. W.; Chong, L. T. *J. Chem. Theory Comput.* **2011**, *7*, 1189-1197.
(38) Hay, B. P.; Rustad, J. R.; Hostetler, C. J. *J. Am. Chem. Soc.* **1993**, *115*, 11158-11164.
(39) Poonia, N. S. *J. Am. Chem. Soc.* **1974**, *96*, 1012-1019.
(40) Live, D.; Chan, S. I. *J. Am. Chem. Soc.* **1976**, *98*, 3769-3778.
(41) Bajaj, A. V.; Poonia, N. S. *Coord. Chem. Rev.* **1988**, *87*, 55-213.
(42) Rodriguez, J. D.; Kim, D.; Tarakeshwar, P.; Lisy, J. M. *J. Phys. Chem. A* **2010**, *114*, 1514-1520.
(43) Martinez-Haya, B.; Hurtado, P.; Hortal, A. R.; Steill, J. D.; Oomens, J.; Merkling, P. J. *J. Phys. Chem. A* **2009**, *113*, 7748-7752.
(44) Martinez-Haya, B.; Hurtado, P.; Hortal, A. R.; Hamad, S.; Steill, J. D.; Oomens, J. *J. Phys. Chem. A* **2010**, *114*, 7048-7054.
(45) Hurtado, P.; Hortal, A. R.; Gámez, F.; Hamad, S.; Martínez-Haya, B. *Phys. Chem. Chem. Phys.* **2010**, *12*, 13752.
(46) Kim, H. J.; Shin, W. J.; Choi, C. M.; Lee, J. H.; Kim, N. J. *Bull. Korean Chem. Soc.* **2008**, *29*, 1973-1976.
(47) Choi, C. M.; Kim, H. J.; Lee, J. H.; Shin, W. J.; Yoon, T. O.; Kim, N. J.; Heo, J. *J. Phys. Chem. A* **2009**, *113*, 8343-8350.
(48) Choi, C. M.; Choi, D. H.; Heo, J.; Kim, N. J.; Kim, S. K. *Angew. Chem. Int. Ed.* **2012**, *51*, 7297-7300.
(49) Inokuchi, Y.; Boyarkin, O. V.; Kusaka, R.; Haino, T.; Ebata, T.; Rizzo, T. R. *J. Am. Chem. Soc.* **2011**, *133*, 12256-12263.
(50) Inokuchi, Y.; Boyarkin, O. V.; Kusaka, R.; Haino, T.; Ebata, T.; Rizzo, T. R. *J. Phys. Chem. A* **2012**, *116*, 4057-4068.
(51) Inokuchi, Y.; Kusaka, R.; Ebata, T.; Boyarkin, O. V.; Rizzo, T. R. *ChemPhysChem* **2013**, *14*, 649-660.
(52) Rodriguez, J. D.; Lisy, J. M. *Int. J. Mass Spectrom.* **2009**, *283*, 135-139.
(53) Rodriguez, J. D.; Vaden, T. D.; Lisy, J. M. *J. Am. Chem. Soc.* **2009**, *131*, 17277-17285.
(54) Rodriguez, J. D.; Lisy, J. M. *J. Am. Chem. Soc.* **2011**, *133*, 11136-11146.

(55) Svendsen, A.; Lorenz, U. J.; Boyarkin, O. V.; Rizzo, T. R. *Rev. Sci. Instrum.* **2010**, *81*, 073107.
(56) Boyarkin, O. V.; Mercier, S. R.; Kamariotis, A.; Rizzo, T. R. *J. Am. Chem. Soc.* **2006**, *128*, 2816-2817.
(57) Rizzo, T. R.; Stearns, J. A.; Boyarkin, O. V. *Int. Rev. Phys. Chem.* **2009**, *28*, 481-515.
(58) Nagornova, N. S.; Rizzo, T. R.; Boyarkin, O. V. *Angew. Chem. Int. Ed.* **2013**, *52*, 6002-6005.
(59) Mohamadi, F.; Richards, N. G. J.; Guida, W. C.; Liskamp, R.; Lipton, M.; Caufield, C.; Chang, G.; Hendrickson, T.; Still, W. C. *J. Comp. Chem.* **1990**, *11*, 440-467.
(60) Frisch, M. J. *et al.*, In *Gaussian 09, Revision A.1*; Gaussian, Inc.: Wallingford CT, 2009.
(61) Kusaka, R.; Inokuchi, Y.; Ebata, T. *Phys. Chem. Chem. Phys.* **2008**, *10*, 6238-6244.
(62) Kusaka, R.; Inokuchi, Y.; Xantheas, S. S.; Ebata, T. *Sensors* **2010**, *10*, 3519-3548.

TOC Figure